

# Analysis of ionospheric irregularities during total solar eclipse 2016 based on GNSS observation

**A Husin, Jiyo, S Anggarani, S Ekawati and V Dear**

Space Science Center, National Institute of Aeronautics and Space Jl. Dr Junjunan 133 Bandung Indonesia.

E-mail: asnawi@lapan.go.id

**Abstract.** A total solar eclipse occurred over Indonesia in the morning hours on 9 March 2016. Ionisations in the ionosphere which is associated with the solar radiation during the total eclipse provided a good opportunity to study the ionospheric irregularities. Using global navigation satellite system (GNSS) data taken from dual-frequency receivers in Manado, we investigated and analysed the total electron content (TEC) perturbations with a time resolution of 60 s to reveal ionospheric irregularities during total eclipse. Result showed that TEC conditions based on IPP were decreased during solar eclipse on March 9, comparing with the neighbour day. The maximum percentage deviation (DTEC) from the average value during eclipse period, 00:00 - 02:40 UT reach -41.5 %. The duration of maximum decrement in TEC occurs were around 2-30 minutes after the maximum obscuration.

## 1. Introduction

Solar eclipse is an interesting phenomena, since it is associated with ionospheric electron densities irregularities. Nevertheless ionospheric response to solar eclipse is quite complex. Studies of ionospheric responses to solar eclipse have been investigated for decades and many authors have been reported. Result in general showed that different regions behave differently during each solar eclipse event. The equipment used and the topic has been widely reported, such as electron density perturbation and wave dynamics in the height of the ionosphere layer during eclipse both in the middle latitudes and lower latitudes as well. At middle latitudes, studies the gravity wave vertical oscillations are raised during solar eclipse [1], response of the ionospheric total electron content (TEC) [2, 3], sporadic E layer (Es) generated during eclipse [4]. At low latitude, some author reported studies ionospheric irregularities during eclipse using ground-based equipment (radar, ionosonde) and satellite based observation (GPS), that provide data with better accuracy both in time and space [5, 6]. In this study, decrease of photo ionization during an eclipse is analysed in comparison with the neighbouring days. The studies done by analysing ionospheric TEC derived from GNSS observation.

## 2. Data and method of analysis.

The data used in this study are from two kind of GNSS receiver, one is the GISTM (*GPS Ionospheric Scintillation and TEC Monitoring*) GPStation-6 receiver Manado (MNDO) and the second is using IGS (International GNSS Service, [https://igs.cb.jpl.nasa.gov/components/dcnav/sopac\\_rinex.html](https://igs.cb.jpl.nasa.gov/components/dcnav/sopac_rinex.html)) Cibonong (BAKO) station which is obtained in the Receiver Independent Exchange (RINEX) format. Table 1 showed the geographic latitude and longitude of both two stations. The ionospheric irregularities behaviour during eclipse analysed by using the temporal evolution of total electron content (TEC)



comparison with the neighbouring days and with particular attention to the satellite at the ionospheric pierce point (IPP) which is about 350 km altitude (figure 2). TEC (1TEC unit, TECU = 10<sup>16</sup> electron m<sup>2</sup>) measurements techniques from GISTM will not be discussed here but it can see in [7] and GNSS data from the IGS processed into TEC using software developed by [8].

The path of lunar umbral shadow moved from the South Sumatra through South Kalimantan, Sulawesi, and Maluku and ended in Pacific Ocean. As shown in figure 1, total eclipse time span start 00:20 UT at south Sumatra, Kalimantan at 00:30 UT, Sulawesi at 00:50 UT, Maluku at 01:00 UT and ended at Pacific Ocean about 01:30 UT. The dashed black line in figure 1, indicated the path of Northern and Southern limit of total eclipse, and the blue solid line is the center path of total eclipse above of the earth surface, <http://eclipse.gsfc.nasa.gov/SEpath/SEpath2001/SE2016Mar09Tpath.html>. While the red solid line is the path of total eclipse at ionospheric height which is converted based on mapping function using ionospheric single layer model (SLM)[9].

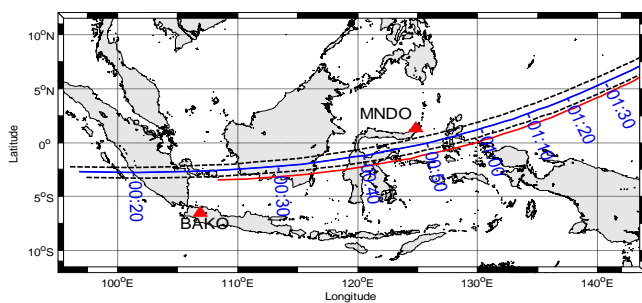


**Figure 1.** Map showing span time the path of maximum obscuration for total solar eclipse of March 9, 2016 (solid blue line) and the red solid line is the path of total eclipse at ionospheric height.

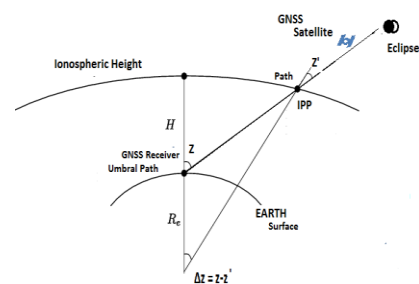


**Figure 2.** Geometry of the single layer model in the sun-fixed coordinate system

The basic geometry of the SLM in the sun-fixed coordinate system shown in figure 2. The signal transmitted from the GNSS satellite to the receiver and umbral shadow as well crosses the ionospheric shell in the so-called ionospheric pierce point (IPP). The zenith angle at the IPP is  $z'$  and the GNSS signal or umbral shadow arrives at the ground station with zenith angle  $z$ . In figure. 2,  $R_e \approx 6,370$  km is the mean Earth radius and  $H$  is the height of ionosphere layer (as single layer, in this study set off 350 km) and the mapping function  $F(z)$  is a triangular function [10] as:

$$F(z) = \frac{1}{\cos z'} = \frac{1}{\sqrt{1 - \sin^2 z'}} \quad (1)$$

The line-of-sight TEC values derived from GNSS signals were converted to vertical TEC values (VTEC) using a mapping function  $F(z)$  in equation 1, and were associated to an ionospheric pierce point latitude and longitude. In similar way for umbral path at ground were associated to latitude and longitude at the peak ionospheric height of 350 km as illustrated in figure 2. The totality of eclipse over Indonesia lasted for a maximum period of about 1.5 minute to 3.5 minute. The eclipse time and percent obscuration at both stations are given in table 1.

**Table 1.** Local circumstances of total solar eclipse on 9 March 2016 at two locations.

Station Name	Station Code	Geographic Latitude	Geographic Longitude	Start of partial eclipse*	Maximum of partial eclipse*	Maximum obscuration*
Cibinong	BAKO	6,49° S	106,85° E	06:19 LT	07:21 LT	88.76%
Manado	MNDO	1.34° N	124.82° E	07:34 LT	08:49 LT	96.66%

\*source: [http://lapan.go.id/files\\_arsip/Info\\_GMT\\_2016.pdf](http://lapan.go.id/files_arsip/Info_GMT_2016.pdf)

The irregularities periods of TEC during eclipse, determined by the detection percentage changes in TEC (% DTEC), which is obtained using the relation in equation 2 [11].

The background TEC for the reference is obtained by averaging the TEC values of 8 and 10 March. These days are considered of a few days before and after the eclipse during the quiet period. The eclipse occurred during the local morning hours and continued for about one and half hour.

$$\%DTEC = \frac{\text{Eclipse day TEC} - \text{Background TEC}}{\text{Background TEC}} \times 100 \quad (2)$$

On the day of eclipse at the observation station, Manado and Cibinong, sky was slightly cloudy but mostly clear and no rainfall. However, two day before solar eclipse, the geomagnetic storm is reported on March 6, 2016. figure 3, show situation of geomagnetic storm before eclipse and scenario to selected data for analysis. As the solar eclipse occurred after the magnetic storm, we safely assume that the results presented in this paper are unaffected by the magnetic storm. Therefore, disturbance storm time index (Dst) data which is taken from world data center for geomagnetism WDC, [http://wdc.kugi.kyoto-u.ac.jp/dst\\_realtime/201603/index.html](http://wdc.kugi.kyoto-u.ac.jp/dst_realtime/201603/index.html), has been used to studies TEC variation during the magnetic storm in order to obtain description storm situation before solar eclipse.

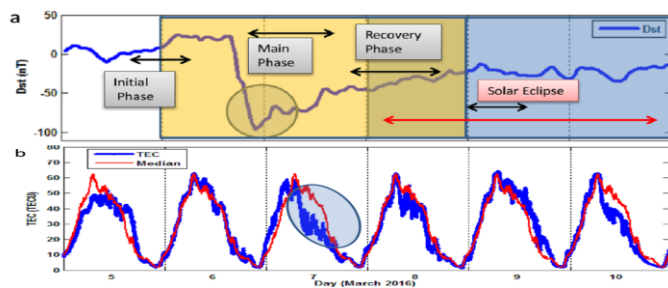


**Figure 3.** a) Dst index indicated moderate geomagnetic storm, before solar eclipse. b) Slight decrease in TEC (blue line) from quiet condition (red line) on March 7 as response of main phase and the next three day, 8, 9 and 10 March are unaffected of magnetic storm.

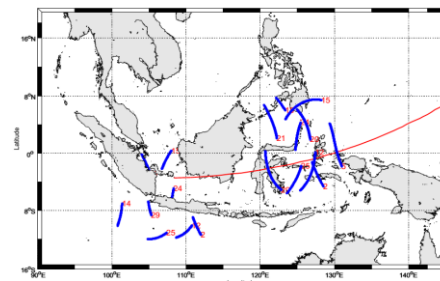


**Figure 4.** Path of all satellites over two stations (blue line) on IPP, along with the path of the maximum obscuration (red line) for period 00:00 UT – 01:00 UT on March 9

### 3. Results

As shown in figure 3, decrease of Dst index (H component) to about -96 nT (moderate storm) that was indicated the main phase of storm occurred on March 6 at 22:00 UT. The initial phase and recovery phase occurred on March 5 and March 7 respectively. TEC variation during geomagnetic storm could be seen in figure 3b. This impact has been studied by analysing TEC of 5, 6, 7, 8, 9 and 10 March from Cibinong (BAKO). The results (figure 3b, shows blue line) reveal a slight decrease in the TEC from its quiet condition (TEC median), in red line, on March 7 as response of main phase. Geomagnetic storm impact on TEC generally occurred only on March 7. However, data used to analysis of solar eclipse to the next three day, 8,9 and 10 March, when recovery phase geomagnetic storm progressing to the rest or quiet condition of the magnetic storm as shown in figure 3. b.

Figure 4, shown path of all satellites on IPP over BAKO and MNDO station, along with the path of the maximum obscuration (red line) for time period 00:00 UT – 01:00 UT, associated to period of solar eclipse event on March 9. The path of the satellite designated by PRN 29, 25, 24, 12, 5 and 2 are crossed the maximum path, while PRN 15, 19, 20 and 21 are slightly distant to the maximum path. These satellites report by MNDO station and selected to analysis of the occurrences of ionospheric irregularities associated with solar eclipse. For satellites report by BAKO station, are continuation of trajectory and mostly distant to the maximum path.

It can be seen in figure 5 that TEC conditions based on IPP were decreased during eclipse March 9, comparing with the neighbour day. The percentage deviation (DTEC) from the average value during eclipse period, 00:00 - 02:40 UT which was calculated by using equation 2, shown in figure 6, for PRN 12, with maximum decrease -40.8 % at 00:54 UT. As shown in figure 6, the vertical total electron content goes on decreasing with time, reach maximum at 00:40 UT (08:40 LT) and after 00:40 UT

starts recovering. The percentage deviation TEC for others satellite which are crossed the maximum path i.e. PRN 29, PRN 25, PRN 24, PRN 5 and PRN 2 respectively -41.5% (00:45 UT), -37%, -29.6 % (01:00 UT), -34.3 % (00:59 UT) and -39.6% (00:46 UT). These results agree with author [3] and [11] by analysis of previous other eclipses.

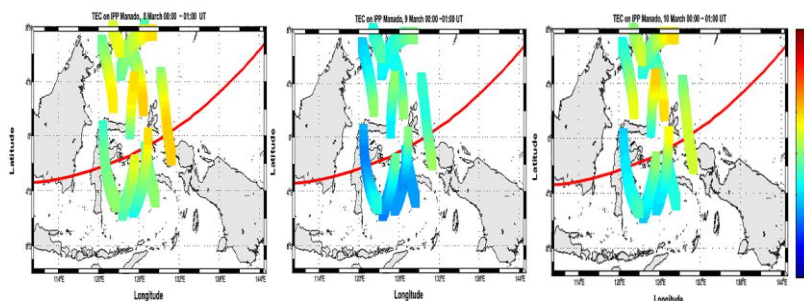


**Figure 5.** TEC conditions based on IPP were decreased during eclipse March 9, comparing with the neighbour day, before and after (March 8 and March 9) period, 00:00 - 01:00 UT

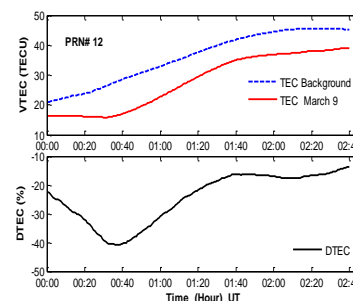


**Figure 6.** Percentage deviation (DTEC) and its evolution of PRN12

According to table 1, the eclipse starts at 07:34 LT and continues for 1 h and 15 min, with the maximum obscuration of 96 % at 08:49 LT (00:49 UT). Daily TEC as background has minimum at pre-dawn and tends to increase gradually with the time of day attaining maximum in the middle day as a result of photoionization due to EUV radiation. However all satellite (PRN) showed the reduction around maximum obscuration during TEC on-going increasing. It is indicated that ionospheric irregularities through TEC decreases during the present obscuration decreases, is directly related to the electron production by decreased photo-ionization process in the ionosphere. It is found that the maximum decrement in TEC occurs about time (2–30 min) after the maximum obscuration.

#### 4. Conclusions

The ionospheric irregularity during the eclipse on 9 March 2016 has been investigated using TEC measurements with particular attention to the satellite at the ionospheric pierce point. The results showed the total ionization, as estimated by the TEC, reduces by approximately maximum -40%. This is generally in agreement with earlier findings for other eclipses. It is found the maximum reduction occurs a few minutes (2–30 min) after the maximum obscuration time. These delay related to timescale in photoionization and transport phenomena.

#### Acknowledgments

The authors would like to acknowledge IGS for GNSS data used and Sam Ratulangi University as collaboration partner.

#### References

- [1] Altadill D, Sole J.G and Apostolov E.M 2001 *J Geophys. Res* **106** 21419-21428.
- [2] Afraimovich E.L, Kosogorov E.A, Lesyuta, O.S 2002 *J Atmos Terr Phys* **64** 1933–1941.
- [3] Jakowski N, Bettac H.D, Lazo B, Palacio L, Lois L 1983. *Physica Solariterrestris* **20** 110–116
- [4] Pezzopane M, Pietrella M, Pignalberi A, Tozzi R 2015 *Adv. Space Res* **56** 2064-2072
- [5] Bagiya, M. S, Iyer K N, Joshi H. P, Thampi S. V, Tsugawa T, Ravindran S, Sridharan R and Pathan B M 2011 *J. Geophys. Res.* **116** A01303
- [6] Kumar S and Singh A K 2012 *Adv Space. Res.* **49** 75 -82,
- [7] Asnawi 2012 *J Aerospace Sciences* **10** 13-22
- [8] Rao P.V.S, Gopi K.S, Niranjan K, and Prasad SVVD 2006 *Ann Geophys* **24** 3279–3292
- [9] Schaer S 1999 Ph.D dissertation Astronomical Institute University of Bern **59**
- [10] Sardon E, Rius A, Zarraoa N 1994 *Radio Sci* **29** 3 577-586
- [11] Kumar S and Singh A K 2012 *Adv Space. Res.* **49** 75 -82,